Processing and characterization of porous alumina scaffolds

SUSMITA BOSE[1], JENS DARSELL[1], HOWARD L. HOSICK[2], LIHUA YANG[3], DIPAK K. SARKAR[3], AMIT BANDYOPADHYAY[1]
[1]*School of Mechanical and Materials Engineering*
[2]*School of Biological Sciences and Molecular Biosciences*
[3]*College of Veterinary Medicine, Washington State University, Pullman, WA 99164-2920, USA*

Bioceramic materials are used for the reconstruction or replacement of the damaged parts of the human body. In this study an improved procedure is described for producing ceramic scaffolds with controlled porosity. Bioinert alumina ceramic was used to make porous scaffolds by using indirect fused deposition modeling (FDM), a commercially available rapid prototyping (RP) technique. Porous alumina samples were coated with hydroxyapatite (HAp) to increase the biocompatibility of the scaffolds. Initial biological responses of the porous alumina scaffolds were assessed *in vitro* using rat pituitary tumor cells (PR1). Both porous alumina and HAp coated alumina ceramics provided favorable sites for cell attachments in a physiological solution at 37 °C, which suggests that these materials would promote good bonding while used as bone implants *in vivo*. Based on these preliminary studies, similar tests were performed with human osteosarcoma cells. Cell proliferation studies show that both the ceramic materials can potentially provide a non-toxic surface for bone bonding when implanted *in vivo*.

1. Introduction

Porous ceramics are good candidate materials for hard tissue engineering. Bone, a natural porous ceramic, is a fascinating organic fibrous material impregnated with small ceramic/mineral crystals (hydroxyapatite, HAp) that provides a structural framework in the body and maintains the positions of various organs. Bone also provides protection for the most vital internal organs and a milieu (via marrow) for the development of the immune system. In the field of bone engineering, it is traditionally the structural aspect of the skeletal system that is considered, along with the biocompatibility of the implanted material. Moreover, because of bone's inherent porous structure, there is a physiological rationale for the use of porous materials as hard tissue scaffolding.

Bioceramic materials have attracted a great deal of interest, for numerous applications by scientists, physicians and engineers, for the last four decades. Such materials can be used for the replacement of hips, knees, teeth, tendons and ligaments, repair for periodontal disease, maxillofacial reconstruction, augmentation and stabilization of the jaw bone, spinal fusion and as a bone filler. In general, bioceramic materials are classified into three broad categories that includes bioinert (such as alumina, zirconia), bioresorbable (such as tricalcium phosphate, TCP) and bioactive (such as HAp bioactive glasses, glass-ceramics). A bioinert material is nontoxic but biologically inactive, whereas a bioactive material is one that elicits a specific biological response at the interface of the biological part and the material, which results in the formation of a bond between the tissues and the material. A biodegradable or bioresorbable substance can break down *in vivo* and the breakdown products are metabolized locally and systemically [1, 2]. In the work described here, alumina, a bioinert ceramic, was used as a scaffold material.

Porous implants with pore sizes in the range of 100–600 μm have been found to be osteoconductive [3]. The advantages of using a porous implant include increased interfacial area between the implant and the tissue which results in less movement of the device in the tissue as well as providing a blood supply to the connective in-grown tissue. Various processing techniques have been utilized to fabricate porous ceramic scaffolds. Most of these processes form structures with randomly arranged pores with a wide variety of sizes, and have limited flexibility to control the pore architecture such as size, distribution or connectivity. The replamineform process is one of these, that has been utilized to fabricate inert, bioactive and polymeric implants via duplicating the porous microstructures of corals that have interconnected pores [4–6]. HAp ceramics have also been fabricated using pore formers or foaming agents that evolve gases during sintering at elevated temperatures [7–9]. During the past decade RP technologies have emerged as revolutionary manufacturing process with the inherent capability to fabricate objects in virtually any shape

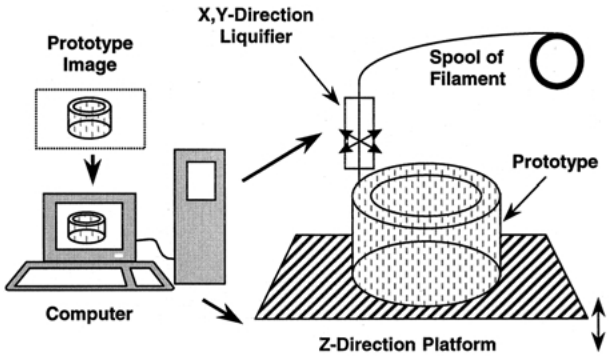

Figure 1 Schematic of the FDM process.

without the need for molds, dies, or tooling. Fused deposition modeling (FDM) is one of the commercially available RP techniques by Stratasys® Inc. (Eden Prairie, MN), in which extruded thermoplastic polymeric filaments are used to build three-dimensional (3D) objects from their computer aided design (CAD) description. The filament passes through a heated liquifier that moves along the *X* and *Y* directions, based on the build strategy of the part to be manufactured. The liquifier extrudes a continuous bead, or road, of material through a nozzle and deposits it on a fixtureless platform. When deposition of the first layer is completed, the fixtureless platform indexes down, and the second layer is built on top of the first layer. This process continues until the fabrication of the part is completed. The temperatures of the liquifier and surrounding environment, as well as filament feed rate and nozzle diameter, are some of the important variables that determine the quality of the final part [10]. Fig. 1 shows the schematic of the FDM process.

In this work, polymeric porous molds that are the negative of the desired ceramic parts are fabricated via fused deposition. The parts are then cast using water based ceramic slurry via the lost mold technique. The paper describes processing and physical characteristics of controled porosity ceramic scaffolds using alumina by indirect FDM process as well as their *in vitro* behavior on two mammalian cell lines.

2. Processing of porous structures

Processing of 3D-honeycomb alumina structures consisted of three stages of development and optimization work. They were (1) mold design and fabrication, (2) development of high solids loaded ceramic slurry composition and (3) binder burn out and sintering cycle development.

Molds were designed and fabricated by FDM 1650 using commercially available ICW-06 thermoplastic wax filament material. Cylindrical molds were designed and fabricated with different raster width and raster gap from 0.62 to 1.1 mm (*x* and *y* gap in Fig. 2a). Top 5 mm of the mold had only perimeter but no raster filling, which is also called lip, to hold excess ceramic slurry during infiltration. Bottom four layers of the mold had no raster gap to avoid leaking of slurry during infiltration. Road width varied from 0.36 to 0.62 mm. Fig. 2b shows schematic of mold architecture and a top view of a mold.

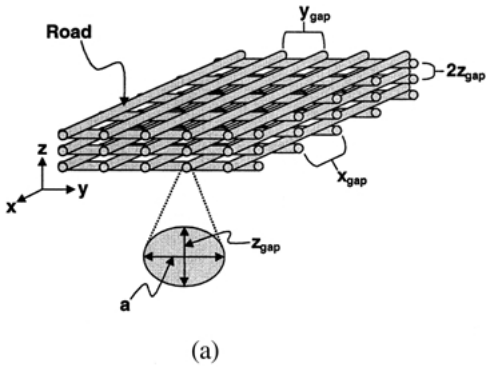

(a)

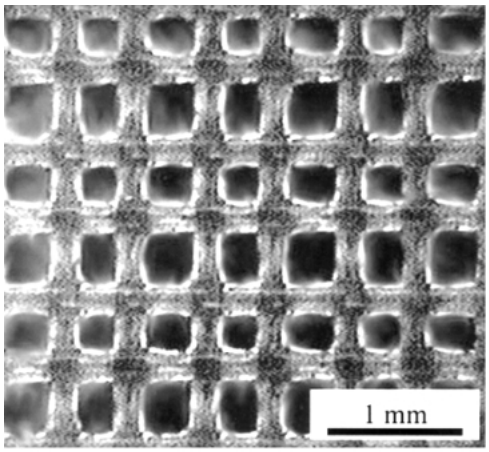

(b)

Figure 2 (a) Schematic and (b) top view of a polymeric mold.

Ceramic slurry development work started with various commercially available high purity alumina powders with different particle size and surface area. Brookfield Viscometer was used to determine the optimum wt % of binder and dispersant needed for the preparation of water based ceramic slurry by measuring the viscosity at different shear rates for each solution. The ideal slurry should have the highest solids loading with the lowest viscosity. The high solids loading help to reduce the shrinkage and related cracking. The low viscosity or high flowability enhance the mold infiltration process and reduce defect concentration due to infiltration. In our experiments, high surface area powder showed higher slurry viscosity compared to low surface area powder at similar solids loading. After screening several powders, 10D alumina powders (Baikowski International Corporation, NC) were selected for this work. The powder was doped with 500 ppm of MgO as a sintering aid, average surface area is $10\,m^2/gm$ and the average particle size (d_{50}) is 0.7 micron. 1-Butanol (Fisher Scientific) was used as an antifoaming agent and Darvan 821 (R.T. Vanderbilt & Co., Norwalk, CT) was used as a dispersant. Fig. 3 shows the variation of slurry viscosity as a function of dispersant amount with respect to shear rate for 10D powders. Alumina powder, antifoaming agent and dispersant were added to water and then ball milled for 5–6 h in a polyethylene bottle. The required amount of binder B-1000 (Rohm and Haas, PA) was added to the mixture just before the infiltration. Polymeric molds, produced via FDM, were then infiltrated with the ceramic slurry. The infiltrated molds

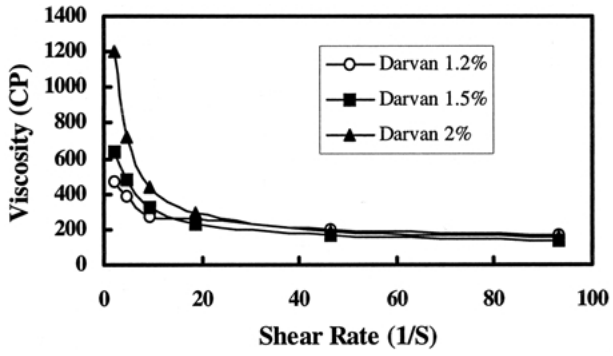

Figure 3 Effect of dispersant amount on the viscosity of ceramic slurry with 10D alumina powders.

were dried at room temperature for two to three days and then subjected to binder removal and sintering cycles.

Binder removal and sintering of infiltrated molds were carried out in a Thermolyne high temperature muffle furnace in furnace air environment. Samples were placed on top of a porous zirconia setter plate. The heating cycle that was used for the binder removal and sintering of alumina ceramics consists of three steps. During the first part of the cycle (at 350 °C), polymeric mold material wicked into the porous zirconia plate and then evaporates at a higher temperature (at 550 °C). At this stage binder leaves the green body. A slower heating rate was used up to 550 °C to avoid cracking or distortion of the part due to binder removal. At higher temperature, densification of alumina ceramic occurs. A final sintering temperature of 1600 °C and a hold time of 3 h was used for all the samples [11].

Fig. 4a shows schematic of a 3D-honeycomb structure and Fig. 4b shows top view of a sintered alumina ceramic structure. The total volume fraction porosity, pore size, pore orientation in the final ceramic structure can easily be varied by changing the road widths and the road gaps in the polymeric molds. For most of the structures, pore sizes were varied between 200 and 600 μm. Mercury intrusion porosimeter plots for some of the porous alumina scaffolds show the distribution of pore volume with respect to pore sizes where most of the pores are concentrated between 150 and 250 μm, which were the desired pore sizes for this structure (Fig. 5). Fig. 5 also shows that keeping the pore size constant, pore volumes alone can be changed. Structures with bimodal or trimodal porosity distribution can also be fabricated by simply changing the starting mold design. Similarly, structures with varying porosity from one end to the other end can be processed using this method. The inherent flexibility of this approach can be utilized to understand the effects of various porosity parameters on biocompatibility and biomechanical properties.

Strength degradation has always been a serious concern in porous ceramic structures. As the total volume fraction porosity increased, the failure strength decreased. Fig. 6 shows uniaxial compression test data of 27–45 vol % porosity samples. Cylindrical porous samples of 10 mm diameter and 15 mm long were tested using an Instron 1331 servo hydraulic machine under stroke control mode at a stroke rate 0.5 mm/min. The failure stress shows an exponential relationship with respect to volume fraction porosity. The final fracture of

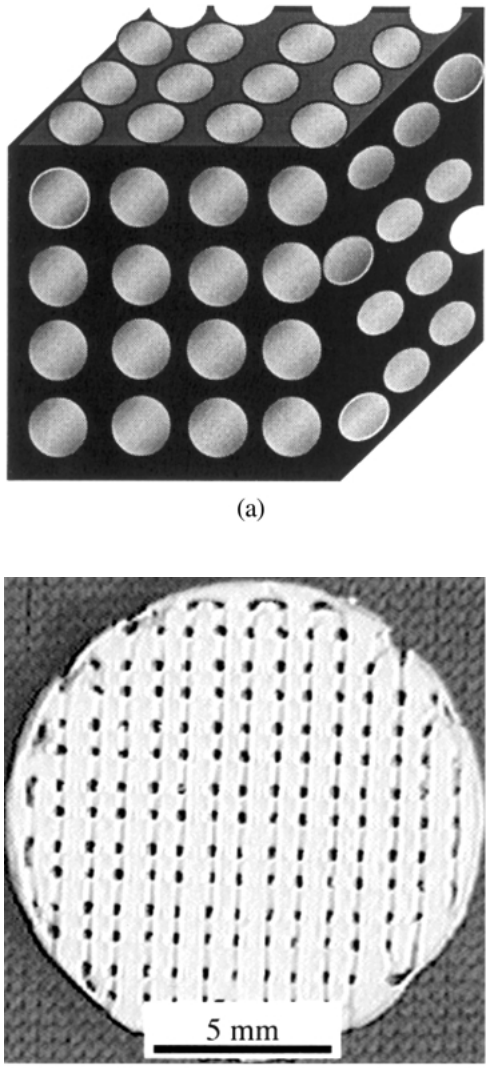

Figure 4 Controlled porosity ceramic scaffolds. (a) A schematic presentation of porous structures. (b) Porous alumina scaffolds of different shapes.

these samples occurred longitudinally along the loading axis with a multifaceted fracture surface [12, 13]. Fig. 7a shows pictures of porous alumina samples having different pore sizes and Fig. 7b shows the gradient

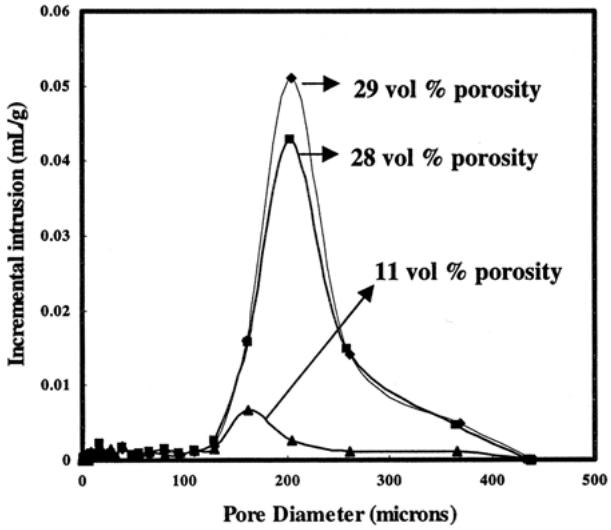

Figure 5 Hg-porosimetry plots show the variations of pore sizes in porous alumina ceramic structures.

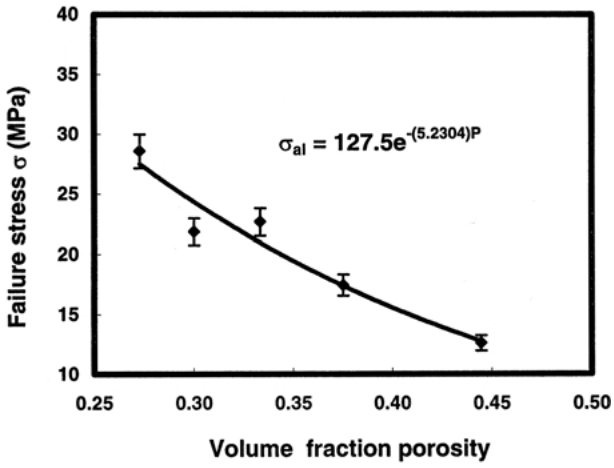

Figure 6 Effects of porosity on compression strength of porous alumina ceramics.

porosity in one sample. It can also be noticed from these samples that not only the internal architecture, but also the external shape of the part can be controlled as in the case of c-ring sample. This is the inherent advantage of the rapid prototyping process where by layer-wise manufacturing, both the micro as well as the macro-structure of the part can be controlled.

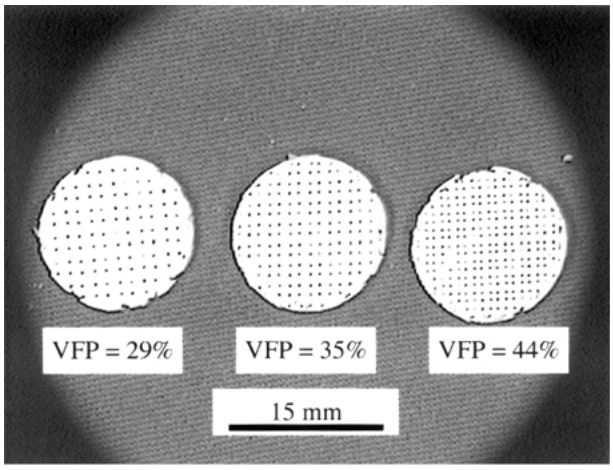

Figure 7a Porous samples with different volume fraction porosity keeping the pore size constant.

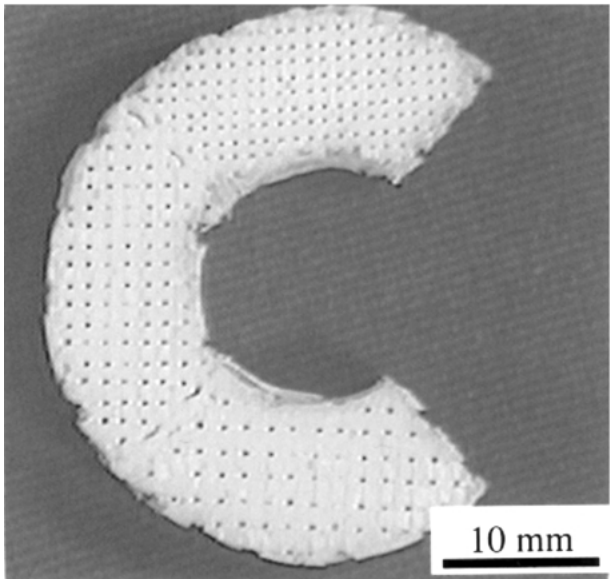

Figure 7b Porous alumina samples with gradient porosity from one end to the other end.

3. Coating of hydroxyapatite (HAp) onto alumina

Alumina is a bioinert material where as HAp is a calcium phosphate based bioactive ceramic. Use of calcium phosphate bioceramics has gained a distinct place in the biomaterials research field during the last two decades. Naturally occurring bone material is primarily calcium phosphate, particularly the calcium phosphates having calcium to phosphorus ratio in between 1.5 and 1.667. TCP (Ca/P = 1.5) and HAp (Ca/P = 1.667) form the boundaries of this compositional range and they are biocompatible, bioactive and osteo-conductive [14–16]. Due to their excellent biocompatibility with living tissue and bone bonding ability these materials have been extensively used for hard and soft tissue repair and replacements and in most instances they support new bone formation when used as micro- or macro-porous biocaramic. In this work HAp was used to coat the porous alumina scaffolds to improve bioactivity. Water based HAp slurry was prepared using HAp powder, 1-Butanol (Fisher Scientific) antifoaming agent and Darvan 821 (R.T. Vanderbilt & Co., Norwalk, CT) diapersant. Porous sintered alumina scaffolds were dipped into the HAp slurry and dried at room temperature for 48 h and then co-fired at 1250 °C for 4 h.

4. Cytotoxicity and cell viability studies on/ in ceramic scaffolds

Alumina ceramics are widely used materials that have found applications in FDA approved bone graft devices. The starting alumina powder is a high purity type suitable for biomedical applications. But during processing of the porous structures, several processing aids are added to the powder. To confirm that these porous structures are non-toxic even after all the processing steps, cytotoxicity and cell viability studies were conducted in tissue culture. Porous alumina ceramic structures and HAp coated alumina ceramic structures were used for this study. Both porous alumina and HAp coated alumina samples were ground to form fine powders to study their cytotoxicity behavior with PR1 cells. After testing the cytotoxicity with PR1 cells, osteosarcoma (SAOS) cells were used for further *in vitro* studies.

For the initial cytotoxicity studies, PR1 cell line was used. This line was derived from a pituitary tumor of an F344 ovariectomized rat treated with estrogen for three months. The tumor cells were grown in culture for 28 generations and then a population of cells showing PRL immunostaining was isolated. These cells were seeded on a 24-well plate in DMEF12 (Sigma) with 2.5% fetal calf serum (FCS, Hyclone Lab.) and 10% horse serum (HS, Hyclone Lab) for 81–85 generations for this study at a density of 2.5×10^5/ml. The culture was incubated at 37 °C in humidified air with 5% CO_2 for 24 h. The medium was replaced every two days carefully during the study. Cells were collected by trypsin and washed two times with the media. The cells were then resuspended in the fresh media and stained with trypan blue to count the

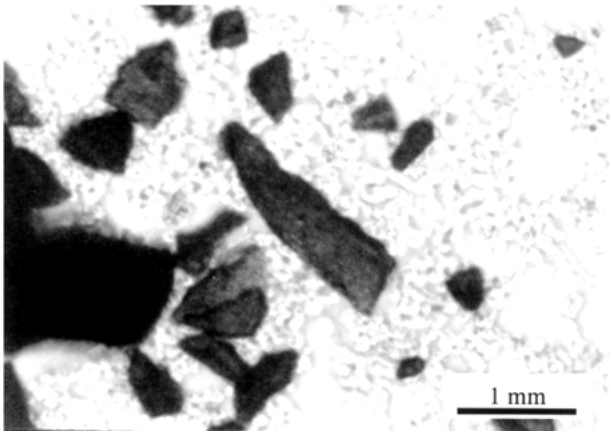

Figure 8 Optical micrograph of alumina in PR1 cells after two days in culture.

viability for two, four and six days. Fig. 8 shows the optical micrograph of the PR1 cells on the surface of alumina after 48 h in culture. A dense cell layer was observed in contact with both the alumina ceramic materials.

5. Cell growth and proliferation

5.1. PR1 cells

Cell proliferation studies were performed with the PR1 cells on alumina and HAp coated alumina samples at different time points. Fig. 9 shows the cell proliferation data for 2 mg samples for two, four and six days comparing control, alumina and HAp coated alumina samples. The HAp coated samples performed a little better than the alumina samples in all the cases. In general, the proliferation was quite comparable for both types of ceramic materials with respect to the performance of the control samples (no ceramic).

5.2. SAOS cells

In order to obtain a preliminary assessment of how cells interact with the scaffolds, we chose to evaluate the properties of a hardy and rapidly growing cell line seeded into various matrices in culture. For this purpose we utilized a human SAOS cell line (SAOS-2 cells, ATCC HTB 85). The cells were cultured in a standard medium made of Dulbecco's modified Eagle's medium supplemented with 10% fetal bovine serum, bicarbonate buffer, 0.01 M Hepes buffer, 100 units/ml penicillin and 100 mg/ml streptomycin. Early passage cells were cultured in the same medium supplemented with 5 ng/ml acidic fibroblast growth factor. The culture was incubated at 37 °C in a humidified 5% CO_2 atmosphere. A calorimetric assay (MTT assay) was used to evaluate cell number at various times after seeding. This assay quantitates the ability of mitochondrial dehydrogenases to metabolize 3-[4,5-dimethylthiazol-2-yl]-2,5-diphenyl-tetrazolium bromide to an insoluble formazan [17]. The amount of formazan is directly proportional to the total number of living cells. This enzyme assay produces a colored product which is quantitated in a microplate reader at $\lambda = 570$ nm. Alumina matrices having 300 micron size pores were tested.

Cells were cultured on two-dimensional (2D) controled porosity alumina ceramic discs (0.1 cm thick and 1 cm diameter) as shown in Fig. 4b. Results described here were obtained with matrices having circular pores 300 μm in diameter. Cells grew well on alumina, after a lag period of a week (Fig. 10). Growth kinetics on alumina was indistinguishable from those on tissue culture plastic surfaces (not shown).

SAOS cells were seeded onto matrices in individual wells of multiwell plates, and onto matrices placed *en masse* in 100 mm bacteriological culture plates. No differences in growth characteristics have been noted. When cells were seeded at densities below 5000 cells/matrix, growth proceeded very little within three weeks. At 10,000 cells/matrix, growth was brisk after about 10 days (Fig. 10), due to a commonly observed ''mass effect'' in cell seeding density.

SAOS cells were grown on alumina matrices for 15 days and then stained for the MTT assay. Before extracting the colored product, scaffolds were viewed with a dissecting microscope (Fig. 11). It is clear that the cells readily colonized this matrix, with cells well distributed along channels, from the surface to channels at the center of the discs. Such observations confirm both the ability of osteoblast-type cells to adhere to this matrix, and also the effectiveness of our technique for seeding and culturing cells within such matrix constructs.

Fig. 12 shows the SEM micrograph of the alumina scaffold that was seeded with SAOS cells to compare cellular morphologies (shape, adhesion, spreading etc.)

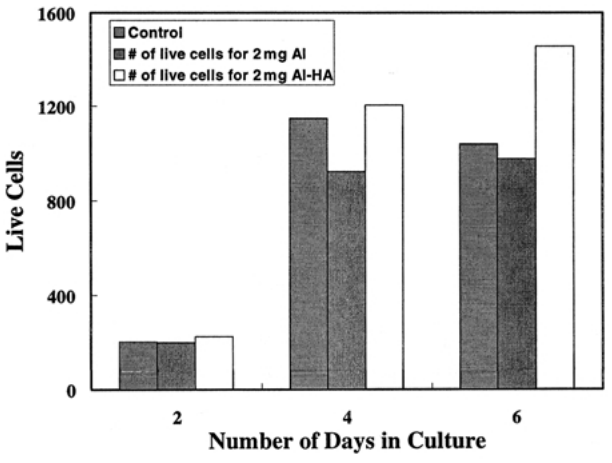

Figure 9 Cell proliferation data for 2 mg alumina and HAp coated alumina samples for two, four and six days in culture.

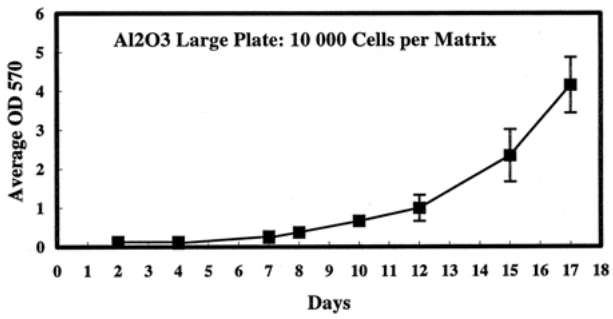

Figure 10 Growth curve on porous alumina scaffold.

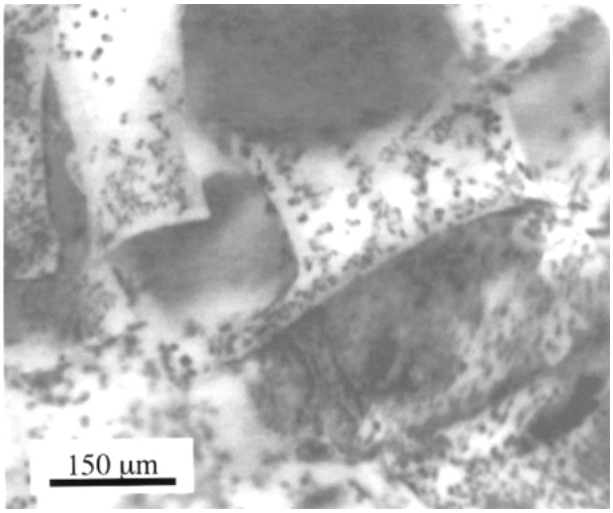

Figure 11 Optical micrograph shows SAOS-2 cells on alumina scaffold.

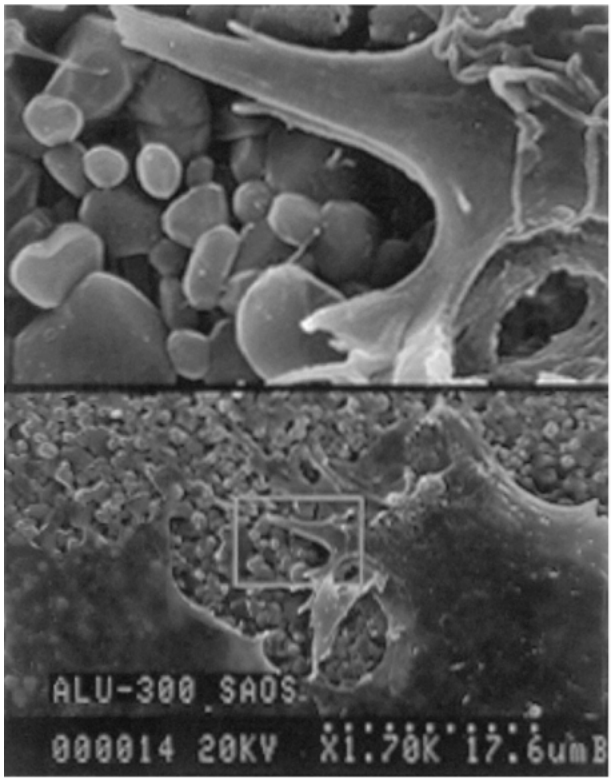

Figure 12 SEM micrograph shows SAOS cells on alumina.

within matrices. It can be observed that the cells spread over the surface, but the impression gained was that cells on alumina stayed on the surface of the granular-appearing matrix, and did not adhere intimately to it. A more intimately adhering cell matrix interaction was found in the case of bioresorbable TCP matrices [18].

6. Conclusions

Controlled porosity 3D-honeycomb porous alumina ceramics have been fabricated using indirect fused deposition process. In this process, not only the internal architecture, but also the shape of the part can be controlled simultaneously. Initial uniaxial compression test data show that as the amount of porosity increases the strength of porous alumina ceramic scaffolds decreases exponentially. From the preliminary *in vitro* test data, it was found that the materials are not toxic after processing and the alumina and HAp coated-alumina provide favorable sites for cell attachment for PR1 and SAOS cells.

Acknowledgments

Authors would like to acknowledge National Science Foundation for the financial support through NSF-CAREER grant DMI 9874971. Experimental support by Raj Atisivan and Ashwin Hattiangadi is also acknowledged.

References

1. (a) L. L. HENCH, *J. Am. Ceram. Soc.* **74** 7 (1991) 1487, (b) S. K. ASHIKU, M. A. RANDOLPH and C. A. VACANTI, *Materials Science Forum,* **250** (1997) p. 129.
2. U. GROSS, R. KINNE, H. J. SCHMITZ and V. STRUNZ, in *CRC Crit. Rev. Biocompat.* **4** (2) (1988).
3. (a) S. F. HULBERT, J. C. BOKROS, L. L. HENCH, J. WILSON and G. HEIMKE, in ''Ceramics in Clinical Applications: Past, Present and Future'', edited by P. Vincenzini (Elsvier, Amsterdam, The Netherlands, 1987), pp. 189–213. (b) S. J. SIMSKE, R. A. AYERS and T. A. BATEMAN, *Materials Science Forum*, **250** (1997) p. 151.
4. E. W. WHITE, J. N. WEBBER, D. M. ROY, E. L. OWEN, R. T. CHIROFF and R. A. WHITE, *J. Biomed. Mater. Res. Symp.* **6** (1975) 23.
5. R. T. CHIROFF, E. W. WHITE, J. N. WEBBER and D. M. ROY, *ibid.* **6** (1975) 29.
6. A. F. TENCER and E. C. SHORS, ''Handbook of Bioactive Ceramics II: Calcium Phosphate and Hydroxylapatite Ceramics'', edited by T. Yamamura, L. L. Hench and J. Wilson (CRC Press, Boca Raton, FL, 1990) pp. 209–21.
7. S. F. HULBERT, S. J. MORRISON and J. J. KLAWITTER, *J. Biomed. Mater. Res. Symp.* **6** (1975) 347.
8. S. F. HULBERT, J. R. MATTHEWS, J. J. KLAWITTER, B. W. SAUER and R. B. LEONARD, *ibid.* **5** (1974) 85.
9. C. P. A. T. KLEIN and P. PATKA, in ''Handbook of Bioactive Ceramics II: Calcium Phosphate and Hydroxylapatite Ceramics'', edited by T. Yamamura, L. L. Hench and J. Wilson (CRC Press, Boca Raton, FL, 1990) p. 53.
10. *Proceedings of Solid Freeform Fabrication*, Austin, TX, August 1992, edited by H. L. Marcus, J. J. Beamen, J. W. Barlow, D. L. Bourell and R. H. Crawford, p. 301.
11. S. BOSE, M. AVILA and A. BANDYOPADHYAY, *Solid Freeform Fabrication Symposium Proceedings*, **9** (1998) 629–636.
12. S. BOSE, S. SUGIURA and A. BANDYOPADHYAY, *Scripta Materialia.* **41**(9) (1999) 1009.
13. A. HATTIANGADI and A. BANDYOPADHYAY, *ibid.* **42** (2000) 181.
14. K. DE. GROOT, *Biomaterials.* **1** (1980) 47.
15. M. JARCHO, *Clin. Orthop. Rel. Res.* **157** (1981) 259.
16. C. J. DAMIEN, J. R. PARSONS, *J. Appl. Biomater.* **2** (1990) 187.
17. P. W. SYLVESTER, H. P. BIRKENFELD, H. L. HOSICK and K. P. BRISKI, *Exp. Cell. Res.* **214** (1994) 145.
18. S. BOSE *et al*. Unpublished work, 2000.

Received 6 June
and accepted 20 December 2000